

# Computer-Aided Design and Optimization of Piezoelectric Ultrasonic Motors

Markus Flueckiger, José M. Fernandez, and Yves Perriard

Integrated Actuators Laboratory - LAI

Ecole Polytechnique Fédérale de Lausanne - EPFL

CH - 1015 LAUSANNE - SWITZERLAND

markus.flueckiger@epfl.ch

**Abstract**—Piezoelectric ultrasonic motors are superior to electromagnetic micro motors, because their efficiency remains theoretically constant during miniaturization. However, the still relatively recent technology has a considerable unexploited optimization potential. Numerical structural analysis by the means of the finite element method (FEM) is a common approach for dimensioning piezoelectric motors. Consequently, there is a need for efficient optimization procedures fitted to the FEM simulation. We developed a dedicated design methodology to first well understand the influence of the geometrical parameters on the movement of the motor. The parameters with the strongest influence on the objective function, the vibration amplitude of the resonator, are used in a following optimization stage. Functional models of rotary and linear motors are built in order to demonstrate their operation. Interferometric measurements validate quantitatively the FEM model along with the suggested design methodology.

## I. INTRODUCTION

Piezoelectric actuators are nowadays established in industrial applications, where their well known advantages make them superior to electromagnetic micro motors. Nevertheless, certain reservations remain. Particularly control and drive electronics are often too complex and thus not economical for many potential application fields. We also observe that the majority of state of the art piezoelectric motors are driven by two or more phase shifted excitation signals [1]. Apart from developments on power electronics for piezoelectric actuators we therefore identify the need for motors with simplified working principles. Those should be controllable by basic electronics comparable to DC motor drives. Consequently we suggest a single phase linear piezoelectric motor, driven by a single low voltage sinusoidal signal.

This paper presents a design methodology for the finite element method (FEM) based development of new piezoelectric motors. It is then applied to linear and rotary piezoelectric motors with the goal of maximizing output speed. This is achieved by optimizing the actuator shape in order to increase the vibration amplitudes that cause the continuous movement. First of all, a parametrization of the motor structure is carried out. Then, with the aim of reducing the number of simulations, but also to limit the variation ranges of the simulation parameters, a preoptimization stage is necessary. Thus, sensitivity analysis is carried out using design of experiments, which is a good way to obtain the influence of the input parameters on the objective function [2]. An optimization study, based on the results from preoptimization, is then realized using the Ansys FEM software [3]. The resonator shapes obtained at each stage

of this optimization process were fabricated and analyzed in order to validate the design methodology.

## II. DESIGN METHODOLOGY

A sensitivity analysis allows for selecting significant system variables of a numerical model. The selected variables are then assigned as free parameters in a FEM based optimization algorithm. The non significant variables are fixed. This restriction of free parameters reduces considerably the computation time necessary for the optimization of any objective function.

### A. Finite Element Method

FEM models approximate the real system. The electrical and mechanical properties are modeled according to (1) and (2) [4].

$$[M] \frac{\partial^2 \{u\}}{\partial t^2} + [C] \frac{\partial \{u\}}{\partial t} + [K_1] \{u\} + [K_2] \{\Phi\} = \{F\} \quad (1)$$

$$[K_2]^T \{u\} + [K_3] \{\Phi\} = \{Q\} \quad (2)$$

where

- $\{u\}$  nodal displacement vector;
- $\{\Phi\}$  electrical potential vector;
- $[M]$  mass matrix;
- $[C]$  damping matrix;
- $[K_1]$  stiffness matrix;
- $[K_2]$  piezoelectric matrix;
- $[K_3]$  dielectric matrix;
- $\{F\}$  nodal mechanical force vector;
- $\{Q\}$  nodal electrical charge vector.

Basically, it would seem judicious to directly maximize output force or speed of the motor by implementing a model of the contact phenomenon between stator and rotor. To reduce model complexity, however, we decided in a first approach to model only the stator. Calculation time for FEM optimization can be significantly reduced in this way. Observing the vibration characteristics allows for conclusions on the output characteristics of the motor.

To model a motor based on the working principle depicted in Fig. 1, the following assumptions were made:

- The piezoceramic actuator is in direct contact and immobile in reference to the resonator. The glue is taken into account by adjusting the damping factor of the resonator system.
- The electrodes glued or soldered on the piezoceramics are not modeled physically. It is supposed that the outer

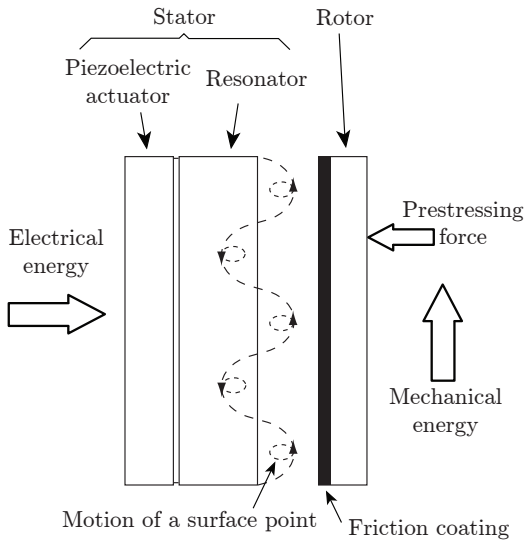


Fig. 1: Working principle of a piezoelectric ultrasonic motor: Electrical energy is converted to mechanical vibration by the means of the converse piezoelectric effect. A friction interface transforms these vibrations to a continuous motion.

surfaces of the piezoceramic are on positive and that the inner surface is on negative electrical potential.

- The surface points of the resonator that are in contact with the rotor are supposed to move freely.

### B. Preoptimization

The objectives of the preoptimization stage are two fold. On the one hand we aim to understand the influence of the different parameters on the objective function. Only those with an important influence are used for the optimization in order

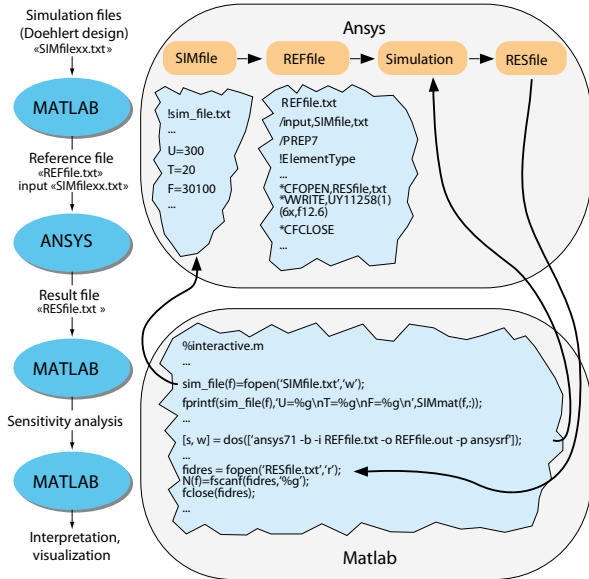


Fig. 2: Steps of the preoptimization procedure

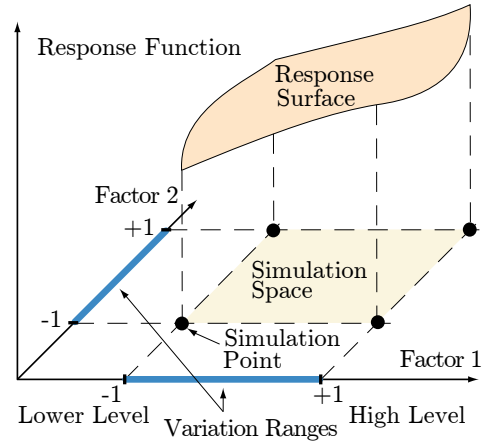


Fig. 3: Response surface analysis illustrated for two factors.

to reduce calculation time. On the other hand the fact to vary the parameter values for the sensitivity analysis leads already to a preoptimized motor design [5]. The steps of the preoptimization are illustrated with Fig. 2 [6].

The sensitivity analysis consists in matching a Taylor series approximation of the response function to the simulation results. We are using a response surface design (Fig. 3) according to Doehlert, which allows to keep small the number of simulations. The equation of the response surface is:

$$Y(x) = a_0 + \sum_{i=1}^N a_i x_i + \sum_{i \neq j}^N a_{ij} x_i x_j + \dots + \sum_{i \neq j \neq k}^N a_{ijk} x_i x_j x_k + a_{i \dots N} x_i \dots x_N \quad (3)$$

With  $k$  system variables,  $n = k(k+1) + 1$  simulations must be executed. In matrix notation, the response function becomes:

$$Y = X A \quad (4)$$

The simulation matrix has the elements  $x_{ij}$ . The  $x_{ij}$  are the simulation value  $x_j$  of the simulation  $i$ .

With the response vector  $Y$  obtained from FEM simulation, the coefficients are calculated:

$$A = (X^T X)^{-1} X^T Y \quad (5)$$

The coefficients  $a_0, a_1, \dots$  are called the effects of the  $x_i$  factors. One makes the distinction between:

- $a_0$  constant effect (equal to the experiments mean),
- $a_i$  main effects,
- $a_{ij}$  effects of the first order interactions,
- $a_{ijk}$  effects of the second order interactions.

### C. FEM Based Optimization

A FEM sweep optimization algorithm implemented in the Ansys software is used to maximize the vibration amplitude and hence the motor speed. The information obtained with sensitivity analysis allowed for using only a restricted set

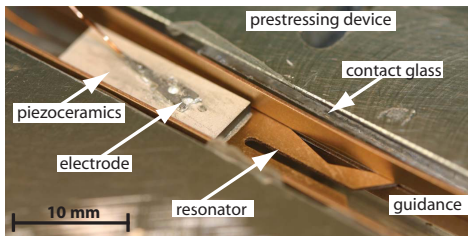
of design variables without affecting the optimization results. Sections III and IV present application examples for linear and rotary motors respectively.

### III. APPLICATION TO A LINEAR MOTOR

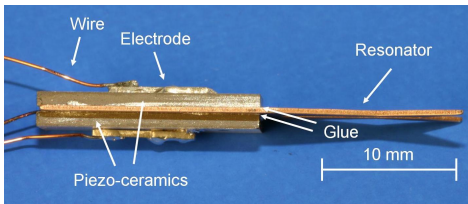
#### A. Working Principle and Modeling

In Fig. 4, a functional model of the linear motor is shown. The actuator is placed within a flexible guidance which at the same time preloads the resonator tips and guides the linear movement of the actuator.

Unlike the motors using the direct working principle [7], the surface points at the resonator tips of the linear motor that are in contact with the guidance do not perform an elliptical movement. Rather, the particular deformation of the resonator corresponds to a pushing or pulling movement respectively. The piezoelectric plates are placed so that the positive potentials are at the exterior surfaces and the negative potential comes into contact with the resonator. This configuration allows for stimulating two of the resonator's Eigen modes at the close by frequencies 84 kHz and 69 kHz. The deformation of the Eigen mode at 84 kHz pushes the actuator forward. At the 69 kHz Eigen mode, the actuator is pulled backward. Particularly, in the first part of a deformation cycle, the resonator tips bend toward the contact. Due to the frictional contact between the resonator tips and the guidance a force is created, that causes the actuator to move in linear direction. When the resonator tips bend away from the guidance during the second part of the deformation cycle, contact is lost. The actuator continues to slide in the same direction because of the relatively high mass of the whole resonator compared to the mass of the tips. This working principle is illustrated in Fig. 5. In the simulations that are displayed by these sequences, the contact was not simulated and the resonator was moving freely. To drive the motor, a single sinusoidal signal is applied to both piezoelectric elements simultaneously in order to excite the

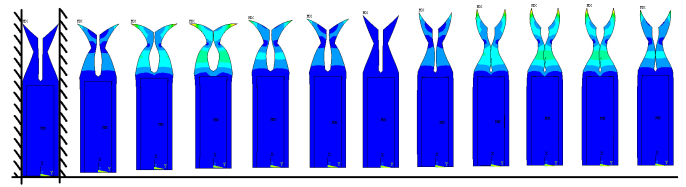


(a)

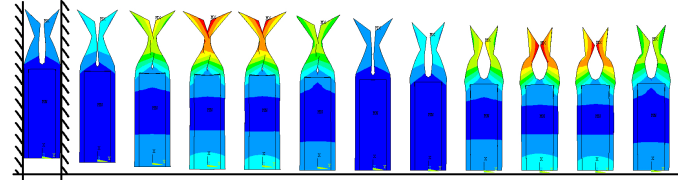


(b)

Fig. 4: a) Functional model of the linear motor. b) Side view of the actuator.



(a) Eigen mode at 84 kHz corresponding to forward movement



(b) Eigen mode at 69 kHz corresponding to backward movement

Fig. 5: Motion sequences of the linear motor. The deformation amplitudes are strongly overdrawn.

resonator's Eigen modes. To change direction, the frequency must be switched between 84 kHz for forward motion and 69 kHz for backward motion.

#### B. Model Validation

Functional models of the linear motor were manufactured at the different stages of the design process.

Firstly, the comparison of simulation results to experimental measurements allowed for improving the numerical model. Because the motor consists of different materials and interfaces between them, the mechanical damping factor is difficult to determine analytically. Hence we started harmonic calculations on the FEM simulation model with an initial guess of 0.2%. Then we used the experimental results from the functional models to adjust the damping factor accordingly. The final simulations were executed with a damping factor of 0.5%.

Secondly, once the FEM simulation model was accurate, the results obtained from the functional models were compared to it and in this manner used to validate the presented design methodology.

Fig. 6 compares the simulated and measured vibration amplitudes:

- Both graphs have qualitatively the same shapes and the same peaks.
- The simulation predicted resonance at about 5% lower frequencies.
- The vibration amplitudes are up to 20% larger in reality. The observed disparity lies within the expected range and is caused by the following effects:
  - Properties of piezoelectric materials are not constant among samples on the one hand and vary with external conditions such as ambient temperature on the other hand.
  - Only a simplified actuator was modeled, which can explain some difference in frequency and the maxima of the deformation amplitude.
  - The mechanical damping factor varies from model to model due to variable piezoelectric properties and manufacturing tolerances.

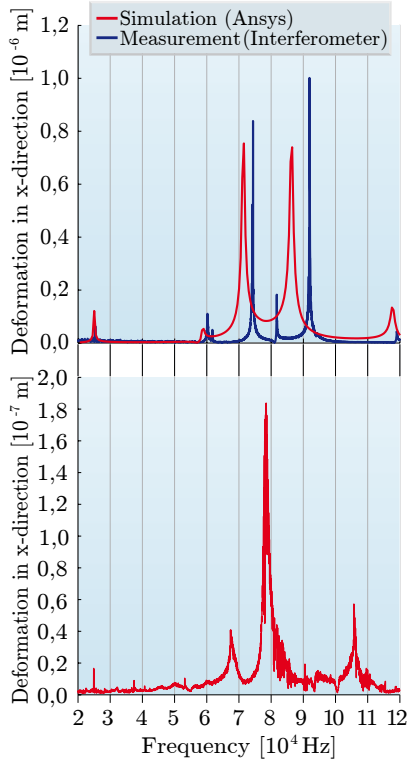


Fig. 6: Deformation amplitude in driving direction. Top: Comparison of the simulated and measured values for the free resonator. Bottom: Measured value for the preloaded resonator.

- During interferometry the movement of the motor was not absolutely free. A small preload was still applied, in order to keep the motor in position.

These observations lead to the conclusion that the experiments did validate the FEM simulations as the results are qualitatively similar and quantitatively very close. No intermediate functional models will be necessary for future designs.

### C. Methodology Validation

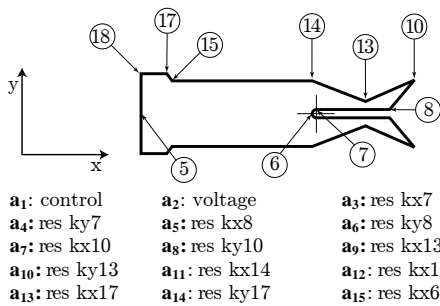


Fig. 7: Definition of the resonator shape. The keypoints correspond to the main effects as indicated. "res k(x,y)i" designates the x and y positions respectively of the resonator keypoint i.

The factors considered for the sensitivity analysis are given in Fig. 7 and the corresponding effects in Fig. 8. The significance threshold is situated at 8%. The design variables with

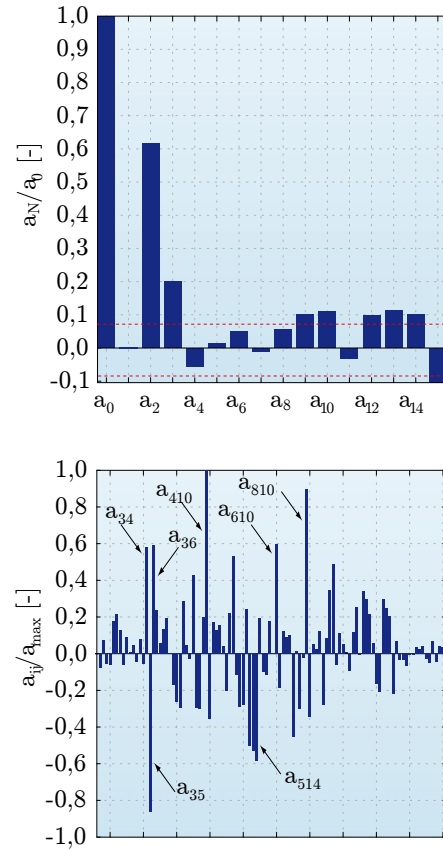


Fig. 8: Sensitivity analysis for the deformation amplitude in driving direction. Top: Main effects. Bottom: Relative effects.

effects  $a_3$ ,  $a_9$ ,  $a_{10}$ ,  $a_{12}$ ,  $a_{13}$ ,  $a_{14}$  and  $a_{15}$  are free for the FEM optimization, the others are fixed.

The methodical resonator shape optimization increased the deformation amplitude of the resonator tips to values up to six times larger compared to the results obtained from the initially guessed resonator shape. Fig. 9 compares the vibration amplitudes at three different stages of the design process. The resonator shapes used for the first FEM simulation,

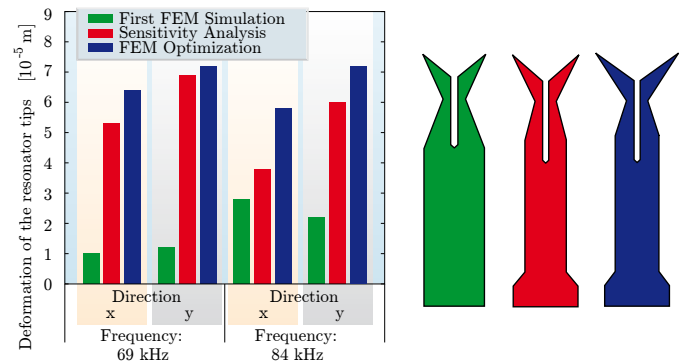


Fig. 9: Comparison of the deformation amplitudes and the resonator geometries at the different stages of the optimization process.

and the ones obtained after preoptimization and after FEM optimization are shown.

#### IV. APPLICATION TO A ROTARY MOTOR

##### A. Working Principle and Modeling

The stator consists of a piezoelectric hollow cylinder with aluminum pushers glued along the cylinder face to operate the contact with the rotor. Fig. 10 shows the arrangement of the pushers, electrode groups and the resulting deformation of the cylinder for excitation of the 3rd tangential-axial mode in the stator [8]. The cylinder is polarized radially. A common drain covers the entire inside surface and two separated electrode groups cover the outside surface. These electrodes allow for excitation of the stator in a special Eigen mode (coupled tangential axial mode) in which the pushers move back and forth at an angle to the end of the cylinder. The number of electrodes in each group is equal to the number of wavelengths around the circumference of the cylinder.

Excitation of the required oscillation mode involves placing a single-phase sine wave voltage on one of the electrode groups. The other group is allowed to float. The rotor is pressed against the pushers by means of a preloading force. Then, due to the oscillations of the stator when excited at the resonant frequency, the pushers impart micro-impulses to the rotor which make it rotate. Rotation in the opposite direction

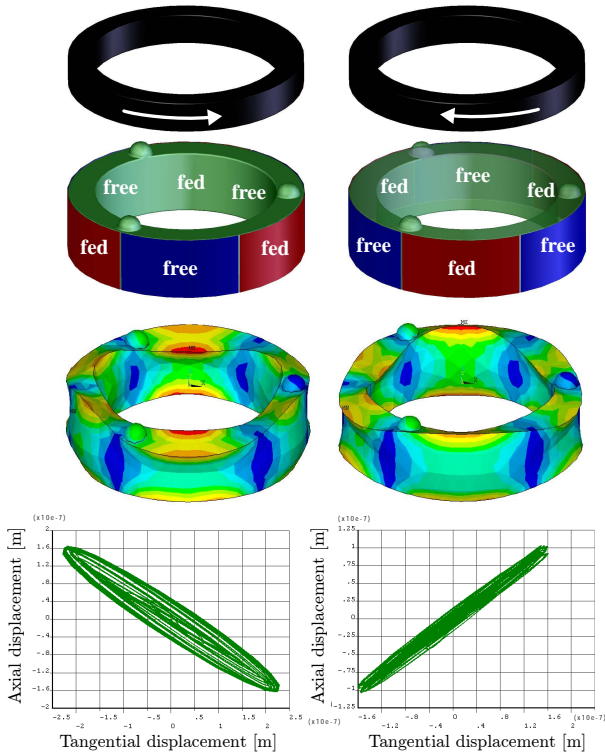


Fig. 10: Working principle of the rotary motor. The vibration mode at the resonant frequency of  $411kHz$  and the corresponding rotor motion is shown; the graphs at the bottom show the corresponding displacement of a surface point. Left: first electrode group active. Right: second electrode group active.

can be obtained by interchanging the roles of the electrode groups.

##### B. Optimization

The system variables considered for sensitivity analysis are:

- $a_0$  Mean
- $a_1$  Outer diameter of piezoceramic
- $a_2$  Inner diameter of piezoceramic
- $a_3$  Thickness of piezoceramic
- $a_4$  Diameter of pusher
- $a_5$  Angle between pushers
- $a_6$  Applied voltage
- $a_7$  Resonant frequency

Fig. 11 shows the normalized main effects corresponding to the Taylor series approximation of the response function. A positive effect signifies that the related factor must be increased in order to maximize the objective function, when the effect is negative, the factor must be decreased.

A larger outer diameter and a smaller inner diameter lead to higher vibration amplitudes. A bigger pusher diameter and a larger angle between them result in higher axial and tangential vibrations, as its obviously true for a higher excitation voltage. However, the conclusion for the material thickness is more difficult. The tangential displacement is bigger for a thinner piezoceramic, whereas the axial displacement is bigger for a thicker piezoceramic. It becomes apparent that we must find a trade-off between optimal axial and optimal tangential

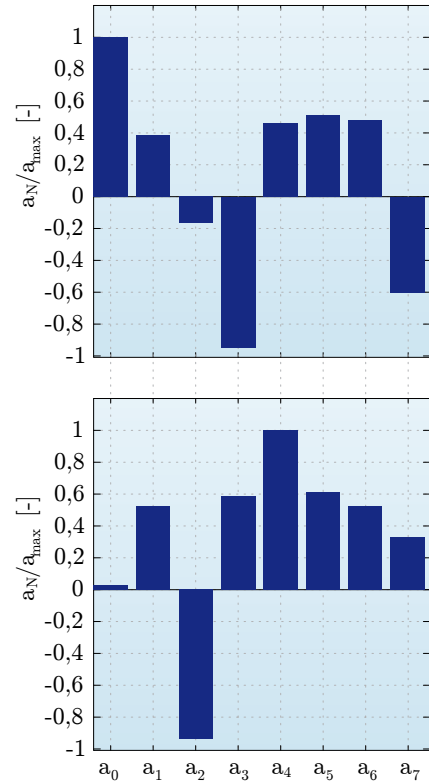


Fig. 11: Main effects for the rotary motor. Top: tangential deformation. Bottom: axial deformation.

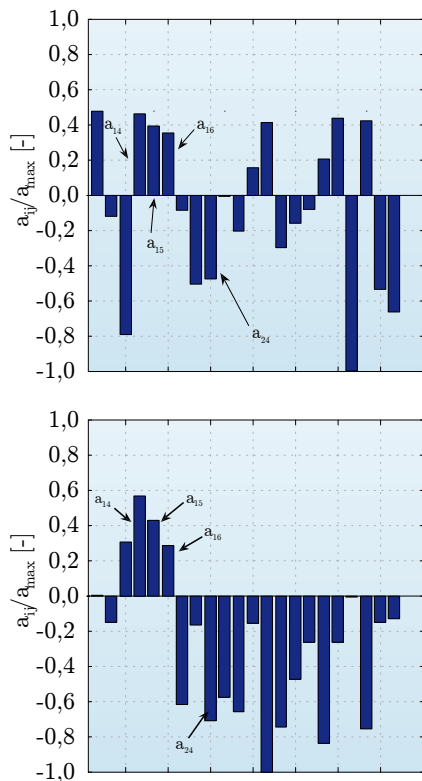


Fig. 12: Relative effects for the rotary motor. Top: tangential deformation. Bottom: axial deformation.

displacement to get an optimal overall behaviour. There the interactions must be considered. In Fig. 12, the relative effects are shown. Looking at the effects which are higher than the threshold for both, axial and tangential deformations, we see that the previous observation is confirmed: increasing outer diameter (relative effects  $a_{14}$ ,  $a_{15}$ ,  $a_{16}$ ) and decreasing inner diameter ( $a_{24}$ ) leads to higher vibrations, whereas the thickness of the ring may be fixed for optimization.

The variation ranges of the free design variables are defined as follows:

15 mm	≤	Outer diameter	≤	15.75 mm
10.9 mm	≤	Inner diameter	≤	11.5 mm
1.5 mm	≤	Pusher diameter	≤	1.575 mm
1.0472 rad	≤	Angle b. pushers	≤	1.0996 rad

The FEM optimization resulted in an increase in axial and tangential vibration amplitudes as illustrated in Fig. 13.

## V. CONCLUSION

The complementary design approach, using design of experiments in a preoptimization stage before applying FEM optimization algorithms to the motor model allows for vibration amplitude maximization. Calculation time of the optimization process is significantly reduced as only significant parameters are used for optimization and others excluded during preoptimization. Furthermore, the variation range of the significant parameters can be narrowed. Functional samples of

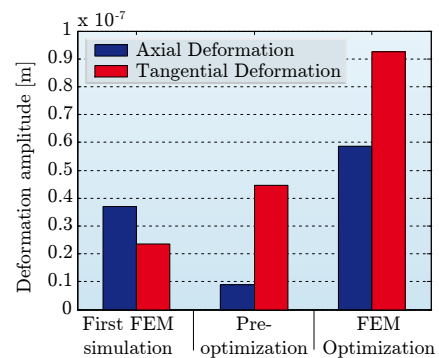


Fig. 13: Evolution of vibration amplitudes during the optimization process for the rotary motor.

linear motors corresponding to the initial, the preoptimized and the optimized structure have been built and tested on an experimental stage. The comparison of their characteristics to the predictions from the FEM model validated the design methodology. It was then successfully applied to a rotary piezoelectric motor with a different working principle.

Nevertheless, an attractive extension would be to implement the contact phenomenon between stator and rotor in the FEM model in order to optimize speed and force output directly. The assumption that bigger deformation amplitudes lead to higher speed and force output does not take into account that output depends not only on the amplitude. The quality of the vibration is indeed very important. The trajectory of a surface point of the resonator under preload, as well as stick and slip phenomena would be interesting to investigate.

## ACKNOWLEDGMENT

The authors would like to thank Claude Amendola at ATPR-EPFL for advice on resonator fabrication as well as Prof. Herbert R. Shea at LMTS-EPFL for his assistance with interferometry.

## REFERENCES

- [1] K. Spanner, "Survey of the various operating principles of ultrasonic piezomotors," in *ACTUATOR 2006, 10th International Conference on New Actuators*, (Bremen), pp. 414–421, June 2006.
- [2] G. Box, W. Hunter, and J. Hunter, *Statistics for Experimenters, An introduction to design, data analysis and model building*. Wiley, 1978.
- [3] Ansys Inc., Canonsburg, PA, *Ansys Multiphysics 8.1 version, User manual*, 2004.
- [4] R. Lerch, "Simulation of piezoelectric devices by two- and three-dimensional finite elements," *IEEE Transactions on Ultrasonics, Ferroelectrics, and Frequency Control*, vol. 37, no. 3, pp. 233–247, 1990.
- [5] J. M. Fernandez and Y. Perriard, "Optimization of a new type of ultrasonic linear motor," *IEEE Transactions on Ultrasonics, Ferroelectrics and Frequency Control*, vol. 55, no. 3, pp. 659–667, 2008.
- [6] J. M. Fernandez and Y. Perriard, "Sensitivity analysis and optimization of a standing wave ultrasonic linear motor," *IEEE Transactions on Ultrasonics, Ferroelectrics, and Frequency Control*, vol. 53, no. 7, pp. 1352–1361, 2006.
- [7] J. Wallaschek, "Piezoelectric ultrasonic motors," *Journal of Intelligent Material Systems and Structures*, vol. 6, no. 1, pp. 71–83, 1995.
- [8] O. Vyshnevskyy, S. Kovalev, and W. Wischnewskiy, "New type of piezoelectric standing wave ultrasonic motors with cylindrical actuators," in *ACTUATOR 2004, 9th International Conference on New Actuators*, (Bremen), pp. 451–455, June 2004.